

Imit Diff: Semantics Guided Diffusion Transformer with Dual Resolution Fusion for Imitation Learning

Yuhang Dong¹ Haizhou Ge² Yupei Zeng¹ Jiangning Zhang³ Beiwen Tian² Guanzhong Tian¹
Hongrui Zhu¹ Yufei Jia² Ruixiang Wang⁴ Ran Yi⁵ Guyue Zhou² Longhua Ma¹

¹Zhejiang University ²Tsinghua University ³Youtu Lab, Tencent
⁴Harbin Institute of Technology, Weihai ⁵ Shanghai Jiao Tong University

Abstract—Visuomotor imitation learning enables embodied agents to effectively acquire manipulation skills from video demonstrations and robot proprioception. However, as scene complexity and visual distractions increase, existing methods that perform well in simple scenes tend to degrade in performance. To address this challenge, we introduce **Imit Diff**, a semantic guided diffusion transformer with dual resolution fusion for imitation learning. Our approach leverages prior knowledge from vision language foundation models to translate high-level semantic instruction into pixel-level visual localization. This information is explicitly integrated into a multi-scale visual enhancement framework, constructed with a dual resolution encoder. Additionally, we introduce an implementation of Consistency Policy within the diffusion transformer architecture to improve both real-time performance and motion smoothness in embodied agent control. We evaluate **Imit Diff** on several challenging real-world tasks. Due to its task-oriented visual localization and fine-grained scene perception, it significantly outperforms state-of-the-art methods, especially in complex scenes with visual distractions, including zero-shot experiments focused on visual distraction and category generalization. The code will be made publicly available.

I. INTRODUCTION

The performance robustness and generalization capabilities of embodied agents in complex manipulation scenarios have long been a focus of significant research interest [17, 47]. Visuomotor imitation learning is one of the mainstream paradigms of robot manipulation policy [6, 40, 48, 9, 13]. This approach enables agents to derive state estimation and decision-making capabilities from expert demonstrations that incorporate high-dimensional visual observations and robot proprioception [49].

However, as scene complexity and visual distractions increase, the performance of decision models that excel in simpler environments tends to degrade [53, 24]. Not only do simple imitation learning policies face challenges, but even advanced multimodal foundation models, such as GPT-4o [16] or vision language action models (VLA) [26, 3, 4, 30, 18, 45], struggle to accurately focus on specific details within semantically complex images. In fact, in robot control and embodied multimodal foundation models, the focus is often on action prediction, observation mapping, or multimodal alignment. Therefore, intuitive visual perception enhancement is typically lacking. Models can only acquire task-oriented semantic localization knowledge from relevant visual regions either implicitly or when guided by high-level text instructions [37].

To tackle this challenge problem, we introduce **Imit Diff**, a diffusion transformer imitation learning framework with dual resolution enhancement guided by fine-grained semantics information. Specifically, our work has three key components:

- 1) **Semantic injection.** **Imit Diff** transforms task-oriented semantic information and high-level textual guidance into explicit pixel-level visual localization labels through the pretrain knowledge of vision language models (VLM) and vision foundation models, and injects them into the policy observation.
- 2) **Dual resolution (dual res) fusion.** We develop a dual res image observation stream and employed a dual res vision encoder to extract global and fine-grained visual features. The extracted multi-scale visual information is subsequently fused within an attention block, integrating fine-grained details into the global visual feature. This approach enhances scene understanding while maintaining computational efficiency.
- 3) **Consistency policy on diffusion transformer (DiT).** Diffusion-based imitation policies often suffer from inefficiencies due to the required denoising steps. To address this, we design a DiT [33] action head incorporating a consistency policy [42], enabling the decision layer to achieve high-frequency system responses through single-step denoising. Furthermore, leveraging faster inference times, we introduce temporal ensemble to enhance the smoothness of predicted actions.

We design four real-world tasks with challenging manipulation precision to evaluate **Imit Diff** and test the model’s scene understanding capabilities by introducing increased scene complexity and visual distractions. Additionally, we conducted zero-shot experiments on visual distraction and category generalization to assess the benefits of the dual res enhancement framework and fine-grained semantic injection. Experimental results demonstrate that **Imit Diff** significantly outperforms existing strong baselines.

In summary, the contributions of our work are three-fold:

- 1) We propose **Imit Diff**, a DiT architecture imitation learning framework with dual res enhancement guided by fine-grained semantics information.
- 2) We developed an open-set vision foundation model pipeline to generate explicit visual masks. This approach effectively addresses challenges such as motion blur,

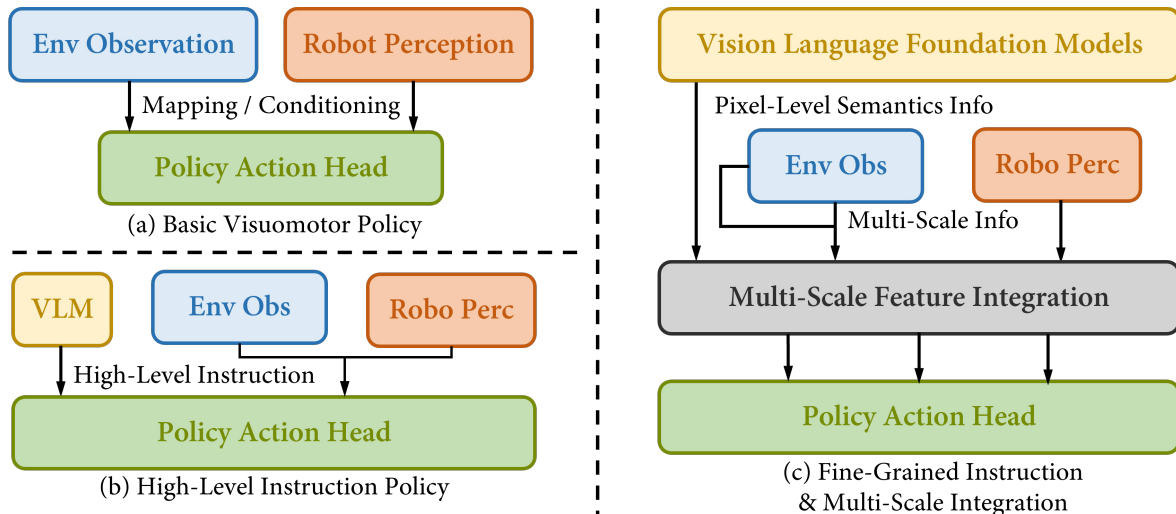


Fig. 1: We compare different visuomotor imitation learning policies: (a) **Basic Visuomotor Policy**, which directly maps or conditions environment observations and robot perception into the action space [51, 19]; (b) **High-Level Instruction Policy**, which incorporates high-level text instruction [27, 37] or motion constraint guidance [14, 31, 20] for the policy through vision language models (VLM); and (c) **Imit Diff**, which transforms high-level instructions into pixel-level semantic information and injects it into a multi-scale visual feature enhancement framework.

occlusion, and object loss in robot control scenarios, leveraging the generated masks as fine-grained semantic information to guide policy decisions.

- 3) We implemented a consistency policy on DiT, which significantly reduced the model inference time. Through the asynchronous control framework, we achieved real-time control under the workflow of open-set vision foundation models.

The code will be made publicly available soon.

II. RELATED WORK

A. Visuomotor Imitation Learning

Imitation learning offers an effective approach for robots to acquire human-like skills through expert demonstrations [44, 1, 12, 38, 10]. Policies based on visual observations have become dominant in the field [32, 11]. These methods focus on mapping or conditioning visual observations to an action space [51, 21]. Recent advancements in diffusion based visuomotor policies have shown significant promise in learning complex manipulation tasks by effectively integrating visual data with high-dimensional, multimodal action distributions [6, 7, 52, 49]. However, these methods focus on the construction of the policy decision layer and lack attention to the visual perception layer in robot manipulation scenarios. In our work, we attempt to propose a dual vision workflow as an enhancement framework for the visual perception layer and inject it with fine-grained pixel-level visual semantic information.

B. Open Vocabulary Vision Foundation Models in Robotics

Multimodal models that integrate vision, language, and action are crucial for developing embodied agents. While

end-to-end approaches are commonly used for offline tasks, learning directly from language-annotated data presents significant challenges, particularly when aligning vision, language observations, and robot sensor data in a shared space [2, 43]. Open vocabulary vision foundation models, including vision language models (VLMs), enable natural language descriptions to guide visual understanding through vision-language joint learning [16, 23]. These models demonstrate strong transferability across various downstream tasks, making them valuable tools in robotics for defining complex objects, serving as semantic anchors for multimodal representations, and providing an intermediate foundation for planning and reasoning. Existing methods, such as VoxPoser [14] and ReKep [15], utilize open vocabulary vision foundation models to acquire high-level text instructions or operational constraints. In our work, we leverage the prior knowledge from these models to align high-level semantic information with fine-grained, pixel-level labels that are the same modality with visual observations.

C. Diffusion Model Acceleration Strategy in Robotics

Diffusion models typically suffer from long inference times due to their iterative sampling process, which presents a key challenge for improving the real-time performance of robot control. Approaches such as Denoising Diffusion Implicit Models (DDiM) [41] and Elucidated Diffusion Models (EDM) [29] interpret the process as a deterministic ordinary differential equation (ODE), reducing inference time by minimizing denoising steps during prediction. However, this variable step size approach reduces the number of denoising steps, which can degrade sampling quality. Other methods, like Picard iteration, accelerate diffusion models through parallel sam-

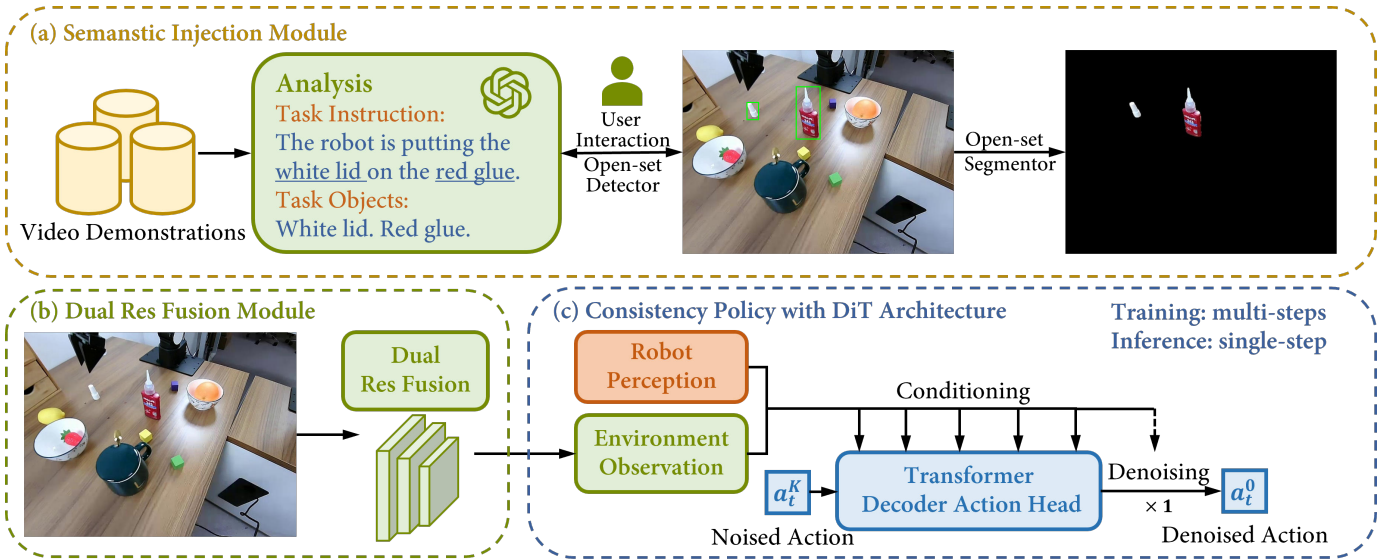


Fig. 2: **Overview of Imit Diff.** We first developed a vision language agent in the (a) **Semantic Injection Module**, where the agent acquires task-oriented semantic descriptions from video demonstrations after interacting with humans. These semantic descriptions are then transformed by the agent into real-time pixel-level visual modality localization labels. The (b) **Dual Res Fusion Module** is responsible for extracting multi-scale visual features from dual res visual observations and fusing them with the previously obtained visual semantic features. The final visual features are then fed into (c) **Consistency Policy with DiT Architecture**, where they serve as environment observations. These features condition the supervision of single-step denoising of actions in the transformer decoder action head together with robot perceptions.

pling, but such approaches are not feasible in computationally constrained robotic systems [39]. Distillation-based techniques enable the student model to take larger steps along the ODE trajectory mapped by the teacher model. Prasad et al. [34] demonstrated this on U-Net, where the student can map inputs with arbitrary step sizes and intervals to the same starting point on the given ODE trajectory. We implement a similar approach in the DiT action head and validate the orthogonality of the consistency policy to the policy structure, resulting in a significant improvement in inference speed.

III. METHOD

Imit Diff is a diffusion transformer imitation learning framework that injects fine-grained semantic information into dual-vision workflows, which extract multi-scale visual features. It also ensures real time control of the robot. To this end, we introduce Imit Diff with three critical components: (a) **Semantics Injection.** Imit Diff injects fine-grained semantic information into policy learning through vision foundation models. (b) **Dual Res Fusion.** The semantic information is then injected into multi-scale vision features extracted by dual res fusion module. (c) **Consistency Policy with DiT Architecture.** Imit Diff constructs a DiT based action head with consistency policy implementation to ensure real time control. An overview of Imit Diff is in Figure 2. We will detail each part in the following sections.

A. Semantic Injection

As shown in Figure 2 (a) Semantic Injection Module, given a manipulation task T (e.g., cover the white lid on the red

glue), we use GPT-4o to analyze the semantic description of the task, considering specified constraints based on user prompts, and filter out objects relevant to the task. We then use the vision foundation model GroundingDINO [25] to add visual cues to the initial frame I_0 . The tracker MixFormerV2 [8] ensures these visual cues are maintained during robot motion, including handling motion blur and occlusion. To balance real-time performance with computational efficiency, we employ Mobile SAM [50] to generate fine-grained visual semantic masks from these visual cues. To maintain alignment, the visual semantic masks are resized to match the low resolution observations in the dual visual streams (which will be described in detail in Section III-B), and the same pre-trained visual encoder is used for domain fine-tuning through different projectors. We integrate a semantic injection block F_S with the transformer decoder architecture to inject visual semantic features I'_S into the visual observation features I'_V , where I'_V are treated as Q , and I'_S as K and V . We do not directly use the visual semantic features as separate observations because we aim for the policy perception layer to learn the relationship between foreground objects and the robot state at the image-level through attention mechanisms.

B. Dual Res Fusion

Imit Diff employs a dual res visual workflow to concurrently extract global features and multi-scale fine-grained features. Figure 3 illustrates this process. The high resolution image $I_H \in \mathbb{R}^{C \times H \times W}$ is first downsampled to a lower resolution $I_L \in \mathbb{R}^{C \times H/2 \times W/2}$. For the low resolution image, the global

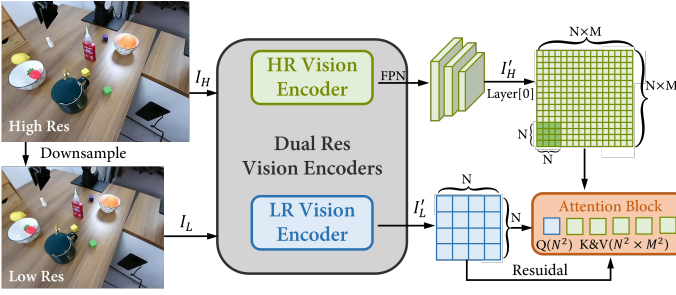


Fig. 3: Illustration of dual res fusion module. The low res workflow extracts global visual information through the vision transformer (ViT), while the high res workflow extracts multi-scale detail information through a convolutional network. In our study, we instantiate low res vision encoder with the CLIP-pretrained ViT-B [35] and high res vision encoder with the LAION-pretrained ConvNext-B [28]. We keep two vision encoders frozen and optimize the projectors for efficient training.

visual feature I_L' are extracted using a vision transformer F_L . For the high resolution image, multi-scale visual feature maps I_{HM} are obtained through a convolutional network F_H . To integrate this multi-scale information and derive fine-grained feature representations, feature pyramid network (FPN) processing is applied to the high resolution visual feature maps. The feature flow processed by FPN yields the bottom-level visual feature $I_H' = I_{HM}^0$, which encapsulates multi-scale fine-grained information by aggregating features from all levels of the pyramid. I_H' is subsequently fused with I_L' via cross-attention within the dual res fusion block. Here, the query (Q) corresponds to $I_L' \in \mathbb{R}^{N^2 \times D}$, while the keys (K) and values (V) are derived from $I_H' \in \mathbb{R}^{N^2 \times M^2 \times D}$. To efficiently leverage visual information across both resolutions, we adopt the sliding window approach inspired by Swin-Transformer, performing patch-level attention fusion. A residual mechanism is incorporated to preserve the original global information prior to fusion. The resulting visual feature I_F is then further integrated with robot perception tokens in the multi-modal fusion block of a transformer encoder structure.

C. Consistency Policy with DiT Architecture

The iterative sampling process of the diffusion model and the pipeline for obtaining visual semantic masks make real time control of the robot a challenge. Inspired by the excellent performance of consistency policy in image generation, we designed a DiT action head based on consistency strategies and integrated it into an asynchronous framework with visual observation acquisition and action prediction. We first train a teacher model G_ϕ within the EDM framework. We then concatenate time t and observation condition o to form the keys (K) and values (V) in the transformer decoder, replacing the FiLM module used in U-Net and input the current action x_t . The derivative of the Probability Flow ODE (PFODE) trajectory is estimated using the attention mechanism:

$$dx_t/dt = -(x_t - G_\phi(x_t, t; o))/t \quad (1)$$

We use an optimized Denoising Score Matching (DSM) loss to train the EDM model. The DSM is sampled along the PFODE trajectory (x_t, t) and is trained to predict the initial action ground truth x_0 .

$$L_{\text{DSM}}(\theta) = \mathbb{E}_{t, x_0, x_t | x_0} [d(x_0, G_\phi(x_t, t; o))] \quad (2)$$

d is an optimized Huber loss:

$$d(x, y) = \sqrt{\|x - y\|_2^2 + c^2} - c \quad (3)$$

For the student model $g_\theta(x_t, t, s; o)$, we concatenate the stop time s with the token sequence of time t and observation condition o , and then denoise the sampled points (x_{t_1}, t_1) and (x_{t_2}, t_2) along the same PFODE trajectory back to the same stop time s . We denote the denoised outputs as $x_s^{(t_1)}$ and $x_s^{(t_2)}$, corresponding to $g_\theta(x_{t_1}, t_1, s; o)$ and $g_\theta(x_{t_2}, t_2, s; o)$, respectively. These are then denoised back to the initial time step $t = 0$, resulting in $g_\theta(x_s^{(t_1)}, s, 0; o)$ and $g_\theta(x_s^{(t_2)}, s, 0; o)$. The consistency loss is then calculated in the fully denoised action space.

$$L_{\text{CTM}} = d\left(g_\theta(x_s^{(t_1)}, s, 0; o), g_\theta(x_s^{(t_2)}, s, 0; o)\right) \quad (4)$$

The final loss calculation combines DSM loss and CTM loss.

$$L_{\text{CP}} = \alpha L_{\text{CTM}} + \beta L_{\text{DSM}} \quad (5)$$

IV. EXPERIMENTS

We present experiments to evaluate the performance of ImIt Diff on fine manipulation tasks. Four real-world tasks are designed to assess ImIt Diff's effectiveness in complex scenes with visual distractions. Ablation experiments highlight the contribution of each component of the policy. Furthermore, zero-shot experiments on visual distraction and appearance / category generalization are conducted to demonstrate that ImIt Diff benefits from the dual visual enhancement framework, which injects fine-grained explicit semantic information.

A. Environment Setup

Robot Setup: ImIt Diff is evaluated across 4 real-world tasks on Airbot Play 6-DoF robot arms, including a teacher and a gripper for demonstration and inference. We use simple RGB web cameras to obtain real-world visual observations from global view and wrist view. Our real-world setup and everyday objects used in our tasks are shown in Figure 4.

Training and Inference Setup: For the four tasks, we use $8 \times \text{A100}$ with 80 GB of VRAM for training all experiments. We use a desktop containing a single 4060 Ti GPU with 16 GB of VRAM for inference.



Fig. 4: **Our robot setup and everyday objects.** We use Airbot Play 6-DoF robot arms including a gripper and a teacher to demonstrate and inference. We also employ diverse everyday objects for our manipulation tasks and visual distraction. Two USB cameras are used to capture global and wrist view visual observations.

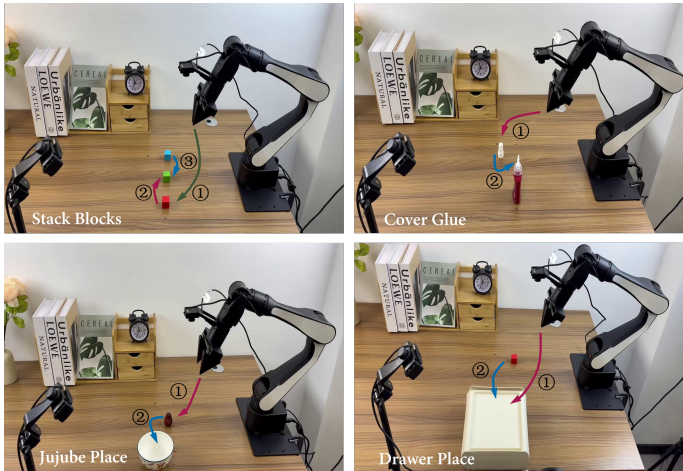


Fig. 5: **Illustrations of all tasks.** We evaluate Imit Diff and baseline methods on four real-world tasks. **Stack Blocks:** (1) grasp the red block, (2) place the red block on the green one, (3) grasp the blue block and place it on the green one. **Cover Glue:** (1) grasp the white lid, (2) insert the white lid onto the red glue. **Jujube Place:** (1) grasp the jujube, (2) place jujube in the bowl. **Drawer Place:** (1) Open the drawer, (2) place the red block into the drawer.

B. Tasks and Metrics

Tasks Setup: We design four real-world tasks with varying manipulation properties and task requirements. Figure 5 illustrates all tasks and we provide detailed explanations of each task’s specific content and the rationale behind our design in the following paragraphs. For all four tasks, we collect 100 demonstrations per task using Airbot Play teleoperation: 50 sets with no visual distraction, 30 sets with easy visual distraction, and 20 sets with hard visual distraction. The different levels of visual distraction are illustrated in Figure 6. A summary of the task setup for Imit Diff is provided in Table I.

TABLE I: **A summary of task setup,** including **Stack Blocks, Cover Glue, Jujube Place** and **Drawer Place** four real-world tasks with different types of manipulation attributes. We collected 100 demonstrations for each task and trained the model with an action horizon of 32. The robot’s perception and actions are based on the joint space poses of the 6DoF arm and gripper.

Real Robot Experiment (4 Tasks)				
Task	Mani	ActH	#Demo	Robo Perc
Stack Blocks	Stack	32	100	Joint
Cover Glue	Insert	32	100	Joint
Jujube Place	Grasp & Place	32	100	Joint
Drawer Place	Hingle	32	100	Joint

- 1) **Stack blocks in order (Stack Blocks).** In this task, the Airbot Play Arm is required to stack three blocks of different colors in a specific order. The stacking operations demand precise alignment to ensure that the blocks do not fall off. This task is designed to assess Imit Diff’s performance on stack manipulation and long-horizon tasks, where fine-grained visual information is crucial for maintaining stability during the manipulation process.
- 2) **Cover white lid on red glue (Cover Glue).** In this task, the Airbot Play Arm is required to first grab the white lid and then place it onto the red glue. This task is designed to evaluate Imit Diff’s performance in insertion-based manipulation, where precise alignment and control are essential for successfully completing the task.
- 3) **Place jujube in bowl (Jujube Place).** In this task, the Airbot Play Arm is required to grab a jujube and place it in a bowl. The task has fine-grained requirements for the grasping position of the jujube to ensure proper placement. This task evaluates Imit Diff’s performance in place-and-grasp manipulation, where precision in both the grasping and placement stages is critical.
- 4) **Place block in drawer (Drawer Place).** In this task, the Airbot Play Arm is required to first open the drawer, then grab the block and place it inside. This task is designed to evaluate Imit Diff’s performance on fine manipulation tasks involving the operation of hinges.

Metrics: For each trained policy, we report average success rates on the policy checkpoint (selected using action mean-squared error). For success rates, we average over 25 trials per situation. Starting positions are randomized between trials for each task.

C. Baselines and Experiment Results

Baselines: We benchmark Imit Diff against state-of-the-art imitation learning policies that have demonstrated significant success in complex robot tasks. Specifically, we use Action Chunking Transformer (ACT) as the baseline model for auto-regression and CVAE, and Diffusion Policy (DP) as the baseline model for diffusion. We use the same action prediction



Fig. 6: **Illustrations of visual distractions level.** Imit Diff can adeptly handle diverse real-world visual scenarios from no distraction to hard distraction.

TABLE II: **Main Results for Real Robot Experiments on Imit Diff and Baselines.** Each task is evaluated with 25 trials. Due to the integration of multi-scale fine-grained visual features and explicit semantic mask injection, Imit Diff demonstrates a strong knowaware of task objects and consistently outperforms other baseline methods in all evaluated tasks.

Algorithm / Task	Stack Blocks			Cover Glue			Jujube Place			Drawer Place		
	Clean	Easy	Hard	Clean	Easy	Hard	Clean	Easy	Hard	Clean	Easy	Hard
Imit Diff	0.80	0.80	0.72	0.96	0.96	0.88	0.96	0.96	0.92	0.88	0.88	0.84
DP (transformer)	0.44	0.20	0	0.32	0.16	0	0.48	0.20	0	0.56	0.32	0
DP (U-Net)	0.40	0.20	0	0.32	0.24	0	0.52	0.20	0	0.56	0.32	0
ACT	0.60	0.32	0	0.76	0.44	0	0.64	0.40	0	0.76	0.52	0

TABLE III: **Ablation study on components of Imit Diff.** We choose Cover Glue as the task for the ablation experiments. The term Multi-Scale indicates whether an FPN (Feature Pyramid Network) is used to extract and fuse multi-scale information from high res visual feature maps. Model-Base refers to the pretrained weights used in the model. Specifically, CLIP-Pretrained means that the low res encoder is a CLIP-Pretrained ViT-B [5], while the high res encoder is a LAION-Pretrained ConvNext-B. On the other hand, DINO-Pretrained means the low res encoder is a DINO-Pretrained ViT-B, and the high res encoder is ConvNext-B.

Low Res	High Res	Multi Scale	Semantic Mask	Model-Base	No Distraction	Easy Distraction	Hard Distraction
✓	✓	✓	✓	CLIP-Pretrained	0.96	0.96	0.88
✓	✓		✓	CLIP-Pretrained	0.56	0.56	0.40
✓	✓	✓		CLIP-Pretrained	0.88	0.60	0.12
✓			✓	CLIP-Pretrained	0.32	0.32	0.24
✓	✓	✓	✓	DINO-Pretrained	0.96	0.92	0.88

horizon for ACT, DP, and Imit Diff. For ACT, we retain the original setup, using images with a resolution of 480×640 (compared to 448×448 for high res and 224×224 for low res in Imit Diff) as the input. For DP, we assign separate CLIP-pretrained ViT-B encoders for both global camera view and wrist camera view, fine-tuning them to ensure the parameter size is consistent with the Imit Diff vision encoder. We evaluate DP based on both U-Net and transformer architectures. For DiT, we omit feature aggregation and maintain full token sequence conditioning, similar to the setup in Imit Diff. We also note that, on the 4060 Ti GPU, the 100-step DDPM variant of DP has an unaffordable inference time per forward pass. Thus we choose the faster and more realistic DDIM, which uses 16 steps for policy inference.

Experiment Results: We conduct experiments on four real-world tasks with three different levels of visual distraction as

shown in Figure 6. The experimental results are summarized in Table II. Imit Diff significantly outperforms the three baseline models, particularly in complex scenes with strong visual distraction. This improvement is attributed to the Dual Res Fusion Module described in Section III-B, which enables Imit Diff to extract multi-scale, fine-grained visual features. Additionally, as discussed in Section III-A, Imit Diff learns distinct task object knowaware through pixel-level Semantic Injection, allowing it to effectively handle visual information in complex scenes and mitigate distraction from irrelevant clutter.

D. Ablation Study

We choose Cover Glue as the reference task for the ablation study. The experimental results are presented in Table III. The ablation study demonstrates the effectiveness of each component in Imit Diff. We utilize two different pretrained

TABLE IV: **Visual Distraction Zero-shot.** We arrange over 10 trials per situation. Imit Diff outperforms baseline models under visual distraction. We note that ACT performs better than DP models due to the z style trained with CVAE.

Algorithm / Task	No Distraction	Easy Distraction	Hard Distraction
Imit diff	0.9	0.9	0.7
ACT	0.8	0.3	0
DP (transformer)	0.6	0	0
DP (U-net)	0.6	0	0

weight models, CLIP and DINO, to achieve the same effective performance, highlighting the transferability of the Imit Diff framework. Additionally, we measured the inference time of different denoising frameworks. We note that due to the occupancy of CUDA by vision foundation models’ inference, EDM takes 1.6s, while the consistency mechanism in the DiT action head (Section III-C) reduces inference time to 0.15s.

E. Zero-shot Generalization Experiment

Distraction Zero-shot Experiment. We collected 100 episodes of data without visual distraction for the Drawer Place task. The goal is to evaluate the robustness of Imit Diff to visual distraction in a zero-shot setting. Table IV presents the comparison of Imit Diff with other baseline methods, demonstrating its superior robustness in handling visual distraction in the zero-shot case.

Appearance & Category Generalization Zero-shot Experiment. Similar to the zero-shot visual distraction experiment, we collected 100 episodes of data without visual distraction for the Drawer Place task. this time we altered the appearance and category of the task objects, as shown in Figure 7. The experimental results are presented in Table V. Imit Diff leverages the explicit fine-grained semantic observations provided by the vision foundation models and the dual res visual enhancement framework, enabling it to achieve superior object appearance and category generalization capabilities.



Fig. 7: **Objects appearance and category generalization of Drawer Place.**

TABLE V: **Appearance & Category Generalization Zero-shot.** We modify the appearance and category of task objects in the Drawer Place environment. Specifically, Appear Grasp and Category Grasp refer to altering the appearance and category of the object to be grasped. Appear Drawer denotes changing the appearance of the drawer.

Algorithm / Task	Appear Grasp	Category Grasp	Appear Drawer
Imit diff	0.8	0.7	1.0
ACT	0.5	0.3	0.8
DP (transformer)	0.5	0.3	0.6
DP (U-net)	0.5	0.2	0.6

V. CONCLUSION

In this work, we present Imit Diff, a fine-grained semantic-guided diffusion transformer imitation learning framework featuring dual res fusion. The core contribution of Imit Diff lies in its innovative utilization of prior knowledge from vision foundation models. It transforms traditionally challenging-to-align high-level semantic supervision into fine-grained semantic masks that share the same modality as visual observations. This pixel-level semantic information is then effectively integrated into the multi-scale visual information extracted by the dual res fusion module. Furthermore, the DiT action head, based on a consistency policy, significantly reduces the denoising time of the diffusion transformer in robot control tasks. Imit Diff demonstrates high accuracy and robustness in fine manipulation tasks, even in complex scenes with visual distractions. Additionally, we showcase the generalization capability of Imit Diff through its performance in zero-shot everyday tasks.

Limitations. Although we have developed an effective visuomotor imitation learning policy, several limitations remain in this work. The open vocabulary vision foundation models pipeline achieves 15-20 FPS on a 4060 Ti GPU, which leaves room for optimization. Future work could explore integrating more advanced and lightweight modules, such as SAM2 [36] or Efficient Track Anything [46], to enhance computational efficiency. Additionally, while the consistency policy improves inference efficiency, its training demands substantial computational resources which introduces instability into training process. Diffusion models based on flow matching may remain for future exploration [22].

REFERENCES

- [1] Ananye Agarwal, Shagun Uppal, Kenneth Shaw, and Deepak Pathak. Dexterous functional grasping. In *7th Annual Conference on Robot Learning*, 2023.
- [2] Kevin Black, Noah Brown, Danny Driess, Adnan Esmail, Michael Equi, Chelsea Finn, Niccolo Fusai, Lachy Groom, Karol Hausman, Brian Ichter, et al. π_0 : A vision-language-action flow model for general robot control. *arXiv preprint arXiv:2410.24164*, 2024.
- [3] Anthony Brohan, Noah Brown, Justice Carbajal, Yevgen Chebotar, Joseph Dabis, Chelsea Finn, Keerthana

- Gopalakrishnan, Karol Hausman, Alex Herzog, Jasmine Hsu, et al. Rt-1: Robotics transformer for real-world control at scale. *arXiv preprint arXiv:2212.06817*, 2022.
- [4] Anthony Brohan, Noah Brown, Justice Carbajal, Yevgen Chebotar, Xi Chen, Krzysztof Choromanski, Tianli Ding, Danny Driess, Avinava Dubey, Chelsea Finn, et al. Rt-2: Vision-language-action models transfer web knowledge to robotic control. *arXiv preprint arXiv:2307.15818*, 2023.
- [5] Mathilde Caron, Hugo Touvron, Ishan Misra, Hervé Jégou, Julien Mairal, Piotr Bojanowski, and Armand Joulin. Emerging properties in self-supervised vision transformers. In *Proceedings of the IEEE/CVF international conference on computer vision*, pages 9650–9660, 2021.
- [6] Cheng Chi, Zhenjia Xu, Siyuan Feng, Eric Cousineau, Yilun Du, Benjamin Burchfiel, Russ Tedrake, and Shuran Song. Diffusion policy: Visuomotor policy learning via action diffusion. *The International Journal of Robotics Research*, page 02783649241273668, 2023.
- [7] Cheng Chi, Zhenjia Xu, Chuer Pan, Eric Cousineau, Benjamin Burchfiel, Siyuan Feng, Russ Tedrake, and Shuran Song. Universal manipulation interface: In-the-wild robot teaching without in-the-wild robots. *arXiv preprint arXiv:2402.10329*, 2024.
- [8] Yutao Cui, Tianhui Song, Gangshan Wu, and Limin Wang. Mixformerv2: Efficient fully transformer tracking. *Advances in Neural Information Processing Systems*, 36, 2024.
- [9] Pete Florence, Corey Lynch, Andy Zeng, Oscar A Ramirez, Ayzaan Wahid, Laura Downs, Adrian Wong, Johnny Lee, Igor Mordatch, and Jonathan Tompson. Implicit behavioral cloning. In *Conference on Robot Learning*, pages 158–168. PMLR, 2022.
- [10] Zipeng Fu, Tony Z Zhao, and Chelsea Finn. Mobile aloha: Learning bimanual mobile manipulation with low-cost whole-body teleoperation. *arXiv preprint arXiv:2401.02117*, 2024.
- [11] Theophile Gervet, Zhou Xian, Nikolaos Gkanatsios, and Katerina Fragkiadaki. Act3d: Infinite resolution action detection transformer for robotic manipulation. *arXiv preprint arXiv:2306.17817*, 2023.
- [12] Siddhant Haldar, Jyothish Pari, Anant Rai, and Lerrel Pinto. Teach a robot to fish: Versatile imitation from one minute of demonstrations. *arXiv preprint arXiv:2303.01497*, 2023.
- [13] Nicklas Hansen, Zhecheng Yuan, Yanjie Ze, Tongzhou Mu, Aravind Rajeswaran, Hao Su, Huazhe Xu, and Xiaolong Wang. On pre-training for visuo-motor control: Revisiting a learning-from-scratch baseline. *arXiv preprint arXiv:2212.05749*, 2022.
- [14] Wenlong Huang, Chen Wang, Ruohan Zhang, Yunzhu Li, Jiajun Wu, and Li Fei-Fei. Voxposer: Composable 3d value maps for robotic manipulation with language models. *arXiv preprint arXiv:2307.05973*, 2023.
- [15] Wenlong Huang, Chen Wang, Yunzhu Li, Ruohan Zhang, and Li Fei-Fei. Rekep: Spatio-temporal reasoning of relational keypoint constraints for robotic manipulation. *arXiv preprint arXiv:2409.01652*, 2024.
- [16] Aaron Hurst, Adam Lerer, Adam P Goucher, Adam Perelman, Aditya Ramesh, Aidan Clark, AJ Ostrow, Akila Welihinda, Alan Hayes, Alec Radford, et al. Gpt-4o system card. *arXiv preprint arXiv:2410.21276*, 2024.
- [17] Yuanchen Ju, Kaizhe Hu, Guowei Zhang, Gu Zhang, Mingrun Jiang, and Huazhe Xu. Robo-abc: Affordance generalization beyond categories via semantic correspondence for robot manipulation. In *European Conference on Computer Vision*, pages 222–239. Springer, 2025.
- [18] Moo Jin Kim, Karl Pertsch, Siddharth Karamcheti, Ted Xiao, Ashwin Balakrishna, Suraj Nair, Rafael Rafailov, Ethan Foster, Grace Lam, Pannag Sanketi, et al. Openvla: An open-source vision-language-action model. *arXiv preprint arXiv:2406.09246*, 2024.
- [19] Seungjae Lee, Yibin Wang, Haritheja Etukuru, H Jin Kim, Nur Muhammad Mahi Shafiqullah, and Lerrel Pinto. Behavior generation with latent actions. *arXiv preprint arXiv:2403.03181*, 2024.
- [20] Xiaoqi Li, Mingxu Zhang, Yiran Geng, Haoran Geng, Yuxing Long, Yan Shen, Renrui Zhang, Jiaming Liu, and Hao Dong. Manipllm: Embodied multimodal large language model for object-centric robotic manipulation. In *Proceedings of the IEEE/CVF Conference on Computer Vision and Pattern Recognition*, pages 18061–18070, 2024.
- [21] Fanqi Lin, Yingdong Hu, Pingyue Sheng, Chuan Wen, Jiacheng You, and Yang Gao. Data scaling laws in imitation learning for robotic manipulation. *arXiv preprint arXiv:2410.18647*, 2024.
- [22] Yaron Lipman, Ricky TQ Chen, Heli Ben-Hamu, Maximilian Nickel, and Matt Le. Flow matching for generative modeling. *arXiv preprint arXiv:2210.02747*, 2022.
- [23] Haotian Liu, Chunyuan Li, Qingyang Wu, and Yong Jae Lee. Visual instruction tuning. *Advances in neural information processing systems*, 36, 2024.
- [24] Ming Liu, Hao Chen, Jindong Wang, and Wensheng Zhang. On the robustness of vision-language models against distractions.
- [25] Shilong Liu, Zhaoyang Zeng, Tianhe Ren, Feng Li, Hao Zhang, Jie Yang, Qing Jiang, Chunyuan Li, Jianwei Yang, Hang Su, et al. Grounding dino: Marrying dino with grounded pre-training for open-set object detection. In *European Conference on Computer Vision*, pages 38–55. Springer, 2025.
- [26] Songming Liu, Lingxuan Wu, Bangguo Li, Hengkai Tan, Huayu Chen, Zhengyi Wang, Ke Xu, Hang Su, and Jun Zhu. Rdt-1b: a diffusion foundation model for bimanual manipulation. *arXiv preprint arXiv:2410.07864*, 2024.
- [27] Xiao Liu, Yifan Zhou, Fabian Weigend, Shubham Sonawani, Shuhei Ikemoto, and Heni Ben Amor. Diff-control: A stateful diffusion-based policy for imitation learning. In *2024 IEEE/RSJ International Conference on Intelligent Robots and Systems (IROS)*, pages 7453–7460.

- IEEE, 2024.
- [28] Zhuang Liu, Hanzi Mao, Chao-Yuan Wu, Christoph Feichtenhofer, Trevor Darrell, and Saining Xie. A convnet for the 2020s. In *Proceedings of the IEEE/CVF conference on computer vision and pattern recognition*, pages 11976–11986, 2022.
- [29] Mang Ning, Mingxiao Li, Jianlin Su, Albert Ali Salah, and Itir Onal Ertugrul. Elucidating the exposure bias in diffusion models. *arXiv preprint arXiv:2308.15321*, 2023.
- [30] Abby O’Neill, Abdul Rehman, Abhinav Gupta, Abhiram Maddukuri, Abhishek Gupta, Abhishek Padalkar, Abraham Lee, Acorn Pooley, Agrim Gupta, Ajay Mandlekar, et al. Open x-embodiment: Robotic learning datasets and rt-x models. *arXiv preprint arXiv:2310.08864*, 2023.
- [31] Mingjie Pan, Jiyao Zhang, Tianshu Wu, Yinghao Zhao, Wenlong Gao, and Hao Dong. Omnimanip: Towards general robotic manipulation via object-centric interaction primitives as spatial constraints. *arXiv preprint arXiv:2501.03841*, 2025.
- [32] Jyothish Pari, Nur Muhammad Shafullah, Sridhar Pandian Arunachalam, and Lerrel Pinto. The surprising effectiveness of representation learning for visual imitation. *arXiv preprint arXiv:2112.01511*, 2021.
- [33] William Peebles and Saining Xie. Scalable diffusion models with transformers. In *Proceedings of the IEEE/CVF International Conference on Computer Vision*, pages 4195–4205, 2023.
- [34] Aaditya Prasad, Kevin Lin, Jimmy Wu, Linqi Zhou, and Jeannette Bohg. Consistency policy: Accelerated visuomotor policies via consistency distillation. *arXiv preprint arXiv:2405.07503*, 2024.
- [35] Alec Radford, Jong Wook Kim, Chris Hallacy, Aditya Ramesh, Gabriel Goh, Sandhini Agarwal, Girish Sastry, Amanda Askell, Pamela Mishkin, Jack Clark, et al. Learning transferable visual models from natural language supervision. In *International conference on machine learning*, pages 8748–8763. PMLR, 2021.
- [36] Nikhila Ravi, Valentin Gabeur, Yuan-Ting Hu, Ronghang Hu, Chaitanya Ryali, Tengyu Ma, Haitham Khedr, Roman Rädle, Chloe Rolland, Laura Gustafson, et al. Sam 2: Segment anything in images and videos. *arXiv preprint arXiv:2408.00714*, 2024.
- [37] Moritz Reuss and Rudolf Lioutikov. Multimodal diffusion transformer for learning from play. In *2nd Workshop on Language and Robot Learning: Language as Grounding*, 2023.
- [38] Mingyo Seo, Steve Han, Kyutae Sim, Seung Hyeon Bang, Carlos Gonzalez, Luis Sentis, and Yuke Zhu. Deep imitation learning for humanoid loco-manipulation through human teleoperation. In *2023 IEEE-RAS 22nd International Conference on Humanoid Robots (Humanoids)*, pages 1–8. IEEE, 2023.
- [39] Andy Shih, Suneel Belkhale, Stefano Ermon, Dorsa Sadigh, and Nima Anari. Parallel sampling of diffusion models. *Advances in Neural Information Processing Systems*, 36, 2024.
- [40] Mohit Shridhar, Lucas Manuelli, and Dieter Fox. Perceiver-actor: A multi-task transformer for robotic manipulation. In *Conference on Robot Learning*, pages 785–799. PMLR, 2023.
- [41] Jiaming Song, Chenlin Meng, and Stefano Ermon. Denoising diffusion implicit models. *arXiv preprint arXiv:2010.02502*, 2020.
- [42] Yang Song, Prafulla Dhariwal, Mark Chen, and Ilya Sutskever. Consistency models. *arXiv preprint arXiv:2303.01469*, 2023.
- [43] Octo Model Team, Dibya Ghosh, Homer Walke, Karl Pertsch, Kevin Black, Oier Mees, Sudeep Dasari, Joey Hejna, Tobias Kreiman, Charles Xu, et al. Octo: An open-source generalist robot policy. *arXiv preprint arXiv:2405.12213*, 2024.
- [44] Chen Wang, Linxi Fan, Jiankai Sun, Ruohan Zhang, Li Fei-Fei, Danfei Xu, Yuke Zhu, and Anima Anandkumar. Mimicplay: Long-horizon imitation learning by watching human play. *arXiv preprint arXiv:2302.12422*, 2023.
- [45] Junjie Wen, Minjie Zhu, Yichen Zhu, Zhibin Tang, Jinming Li, Zhongyi Zhou, Chengmeng Li, Xiaoyu Liu, Yaxin Peng, Chaomin Shen, et al. Diffusion-vla: Scaling robot foundation models via unified diffusion and autoregression. *arXiv preprint arXiv:2412.03293*, 2024.
- [46] Yunyang Xiong, Chong Zhou, Xiaoyu Xiang, Lemeng Wu, Chenchen Zhu, Zechun Liu, Saksham Suri, Balakrishnan Varadarajan, Ramya Akula, Forrest Iandola, et al. Efficient track anything. *arXiv preprint arXiv:2411.18933*, 2024.
- [47] Zhecheng Yuan, Tianming Wei, Shuiqi Cheng, Gu Zhang, Yuanpei Chen, and Huazhe Xu. Learning to manipulate anywhere: A visual generalizable framework for reinforcement learning. *arXiv preprint arXiv:2407.15815*, 2024.
- [48] Yanjie Ze, Ge Yan, Yueh-Hua Wu, Annabella Macaluso, Yuying Ge, Jianglong Ye, Nicklas Hansen, Li Erran Li, and Xiaolong Wang. Gnfactor: Multi-task real robot learning with generalizable neural feature fields. In *Conference on Robot Learning*, pages 284–301. PMLR, 2023.
- [49] Yanjie Ze, Gu Zhang, Kangning Zhang, Chenyuan Hu, Muhan Wang, and Huazhe Xu. 3d diffusion policy. *arXiv preprint arXiv:2403.03954*, 2024.
- [50] Chaoning Zhang, Dongshen Han, Yu Qiao, Jung Uk Kim, Sung-Ho Bae, Seungkyu Lee, and Choong Seon Hong. Faster segment anything: Towards lightweight sam for mobile applications. *arXiv preprint arXiv:2306.14289*, 2023.
- [51] Tony Z Zhao, Vikash Kumar, Sergey Levine, and Chelsea Finn. Learning fine-grained bimanual manipulation with low-cost hardware. *arXiv preprint arXiv:2304.13705*, 2023.
- [52] Tony Z Zhao, Jonathan Tompson, Danny Driess, Pete Florence, Kamyar Ghasemipour, Chelsea Finn, and

- Ayzaan Wahid. Aloha unleashed: A simple recipe for robot dexterity. *arXiv preprint arXiv:2410.13126*, 2024.
- [53] Jinliang Zheng, Jianxiong Li, Sijie Cheng, Yanan Zheng, Jiaming Li, Jihao Liu, Yu Liu, Jingjing Liu, and Xi-anyuan Zhan. Instruction-guided visual masking. *arXiv preprint arXiv:2405.19783*, 2024.